

Multifractality and intermediate statistics in quantum maps

J. Martin, O. Giraud and B. Georgeot

Laboratoire de Physique Théorique, Université de Toulouse, CNRS, 31062 Toulouse France

(Dated: February 9, 2022)

We study multifractal properties of wave functions for a one-parameter family of quantum maps displaying the whole range of spectral statistics intermediate between integrable and chaotic statistics. We perform extensive numerical computations and provide analytical arguments showing that the generalized fractal dimensions are directly related to the parameter of the underlying classical map, and thus to other properties such as spectral statistics. Our results could be relevant for Anderson and quantum Hall transitions, where wave functions also show multifractality.

PACS numbers: 05.45.Mt, 05.40.-a, 05.45.Df, 71.30.+h

Statistical properties of wave functions and energy levels of quantum systems have been an important topic of research in the past decades with many applications to physical systems. It is now well-known that energy levels of e.g. quantum systems whose classical limit is chaotic, or disordered systems when eigenstates are extended, follow Random Matrix Theory (RMT). In this case, wave functions are typically ergodic and level statistics show level repulsion at short distances. Conversely, systems whose classical limit is integrable, or disordered systems in a regime of Anderson localization, show Poisson statistics of energy levels (without level repulsion), and wave functions are typically localized in phase space [1].

It has been realized only later that another universality class exists which is intermediate between the latter two. It can be observed in disordered systems at the Anderson transition [2], or in certain systems whose classical limit is pseudo-integrable [3]. In this case, level statistics follow specific laws called semi-Poisson statistics, and wave functions generally show multifractal properties. This multifractal behavior has been extensively studied in the case of the Anderson transition [4, 5, 6], and has been also seen in quantum Hall transitions [7].

Recently, a simple model for intermediate systems was introduced which corresponds to a quantization of a certain interval-exchange map [8]. The model, although very simple, can display the whole range of semi-Poisson statistics when a parameter is changed. Moreover, a certain randomization of this system was shown to yield a new model of Random Matrices with intermediate statistics [9].

Here, we examine multifractal properties of eigenfunctions for the Random Matrix model corresponding to intermediate quantum maps. We compute the inverse participation ratios (IPR), fractal dimensions, and singularity spectra in a variety of regimes with different numerical methods. Using extensive numerical studies and analytical arguments, we show that the parameter of the model can be related to the fractal dimensions of the eigenfunctions, as well as to the spectral statistics. This Random Matrix model is known to span the whole range of semi-Poisson statistics for both short-range and

long-range statistics. Thus our results indicate with some generality the existence of a link between the statistics of eigenvalues and the multifractal properties of the eigenfunctions.

Let us start with the classical map defined on the 2-torus by $\Phi_\gamma : \bar{p} = p + \gamma \pmod{1} ; \bar{q} = q + 2\bar{p} \pmod{1}$, where (p, q) , the coordinates in phase space, are the conjugated action and angle variables and the bars denote the resulting variables after one iteration of the map. The quantization of this map yields a unitary evolution operator acting on a Hilbert space of dimension $N = 1/(2\pi\hbar)$ which can be expressed in momentum space by the $N \times N$ matrix [8, 9]

$$U_{pp'} = \frac{e^{i\phi_p}}{N} \frac{1 - e^{2i\pi N\gamma}}{1 - e^{2i\pi(p-p'+N\gamma)/N}}, \quad (1)$$

with $\phi_p = -2\pi p^2/N$. From this quantized map one can construct an ensemble of random matrices, taking ϕ_p as random variables uniformly distributed in $[0, 2\pi[$ [9]. The statistical properties of the pseudo-spectrum (the set of eigenphases) of U strongly depend on the value of the parameter γ . On the one hand, for generic irrational γ , the spectral statistics of U are expected to follow those of the Circular Unitary Ensemble (CUE) of RMT if the ϕ_p are independent (non-symmetric case), or the Circular Orthogonal Ensemble (COE) if one imposes a symmetry $\phi_{N-p} = \phi_p$. On the other hand, for rational $\gamma = a/b$, a variety of different behaviors are observed [8]. It was shown in [9] that for $aN = \pm 1 \pmod{b}$ the spectral statistics is of semi-Poisson type. In particular the nearest-neighbor spacing distribution is given by $P_\beta(s) = A_\beta s^\beta e^{-(\beta+1)s}$ with parameter $\beta = b - 1$ in the non-symmetric case ($\beta = b/2 - 1$ in the symmetric case). For $aN \neq \pm 1 \pmod{b}$, $P(s)$ is still of intermediate type but with more complicated formulas [10]. Finally when γ is an integer the eigenphases are equally spaced and the spectrum is totally rigid. Thus the set of quantum maps U with rational γ gives a random matrix ensemble with intermediate statistics (ISRM) whose spectral statistics correspond to natural intermediate distributions between Poisson and RMT, controlled by the value of γ .

Multifractality properties of wave functions are de-

scribed by a whole set of generalized fractal dimensions D_q . For a vector $|\psi\rangle = \sum_{i=1}^N \psi_i |i\rangle$ in an N -dimensional Hilbert space, the multifractal exponents D_q are defined through the scaling of the moments

$$\sum_{i=1}^N |\psi_i|^{2q} \propto N^{-D_q(q-1)}. \quad (2)$$

The fractal dimension for $q = 0$ corresponds to the dimension of the support of the measure, here $D_0 = 1$. The fractal exponent D_2 describes the large-size behavior of the IPR $\xi = 1/\sum_{i=1}^N |\psi_i|^4$, which measures the extension of the state $|\psi\rangle$ over the basis vectors. The multifractal exponents describe the behavior of the partition function

$$Z(q, L) \equiv \sum_{k=1}^{N_b} \mu_k(L)^q \propto L^{\tau_q}, \quad \tau_q \equiv D_q(q-1), \quad (3)$$

where the vector $|\psi\rangle$ is divided into $N_b = N/L$ boxes B_k of size L , and $\mu_k(L) = \sum_{i \in B_k} |\psi_i|^2$, $1 \leq k \leq N_b$. The multifractal properties are alternatively characterized by the singularity spectrum $f(\alpha)$, which is the fractal dimension of the set of points whose singularity exponent is α . It is related to the function τ_q by a Legendre transform. Introducing the normalized measures $\mu_k(q, L) = \mu_k(L)^q / \sum_i \mu_i(L)^q$, the singularity exponent and the associated fractal dimension can respectively be obtained by [11]

$$\begin{aligned} \alpha(q) &= \frac{d\tau_q}{dq} = \lim_{L/N \rightarrow 0} \frac{\sum_i \mu_i(q, L) \log \mu_i(L)}{\log(L/N)}, \\ f(\alpha(q)) &= q\alpha(q) - \tau_q = \lim_{L/N \rightarrow 0} \frac{\sum_i \mu_i(q, L) \log \mu_i(q, L)}{\log(L/N)}. \end{aligned} \quad (4)$$

Let us consider an ensemble of matrices of type (1) with rational $\gamma = a/b$, in the non-symmetric case where all ϕ_p are independent. The mean IPR for eigenvectors of these matrices in p representation for different values of γ with denominator $b = 7$ is displayed in Fig. 1 as a function of the matrix size. The IPR scales as N^{D_2} provided data corresponding to different values of $aN \bmod b$ be treated separately. Indeed, when different matrix sizes are grouped into families, the results yield a linear behavior of $\log(\xi)$ as a function of $\log N$, with the same slope D_2 for each family. More generally we observed that the fractal exponents D_q are well defined if data are organized into families, and that they only depend on the denominator b of γ .

We now proceed to compute the fractal exponents D_q . A few of these exponents have already been computed in [9, 12] for the case $aN \equiv \pm 1 \bmod b$. Here our aim is to characterize D_q as a function of q . The quantities D_q and $f(\alpha)$ are known to be difficult to compute numerically, especially for large q or α . In this work, we resorted to several different methods as a consistency check. We first opted for the usual method of moments. We computed

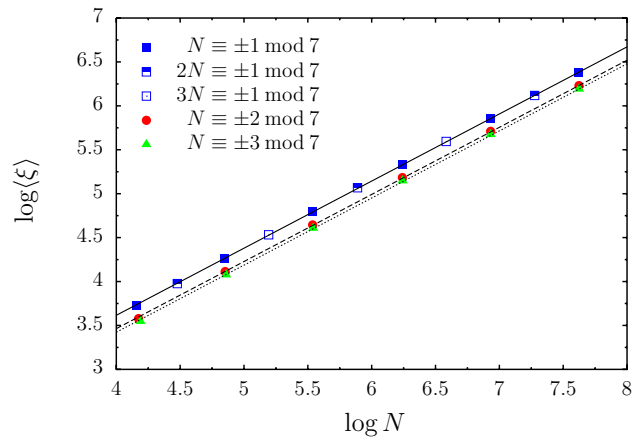


FIG. 1: (Color online) Mean IPR of eigenvectors of (1) as a function of the vector size N for $\gamma = a/b$ with $b = 7$ and $a = 1$ (filled symbols), $a = 2$ (half-filled squares), $a = 3$ (empty squares). Straight lines correspond to the best linear fits. Logarithm is natural.

average values of the moments (2) for different system sizes N ranging from ~ 2000 up to ~ 12000 to get rid as much as possible of finite size effects [13]. The fractal dimensions are extracted from the slopes of the graphs of $\log(\sum_i |\psi_i|^{2q})$ versus $\log N$. Here the average is taken over all eigenvectors and random realizations of U (from 200 realizations for $N \sim 2000$ to 1 for $N \sim 12000$). We also opted for the so-called canonical method [11] allowing to determine the $f(\alpha)$ spectrum directly from Eq. (4). For this method, the numerical computations were done on a single realization of size $N \sim 13000$, and 20 box sizes ranging from $L = 10$ to $L = 0.1N$ (again different families of box sizes were treated separately). We also considered other approaches, such as the box counting method based on Eq. (3); they all give results intermediate between the two previous methods.

The results for D_q are displayed in Fig. 2. For increasing b , the curve for D_q tends slowly to the limiting curve where $D_q = 1$ for all q , which corresponds to non-fractal wave functions. This is in agreement with the fact that γ tends for $b \rightarrow \infty$ to an irrational number for which the system is expected to follow RMT. Figure 2 shows that D_q is roughly linear in a relatively large interval around $q = 0$, and tends to limiting values $D_{\pm\infty}$ for large $|q|$. The slope of D_q at $q = 0$ is displayed in the inset of Fig. 3 as a function of b . We found that the value of this slope is very accurately given by $-1/b$. Since $D_0 = 1$, the first-order expansion of D_q around $q = 0$ reads

$$D_q \approx 1 - \frac{q}{b}. \quad (5)$$

This expansion turns out to be valid in a quite large interval of q , whose size increases with b . As an example, the numerical values of D_1 and D_2 together with the linear approximation (5) are shown in Fig. 3. When b

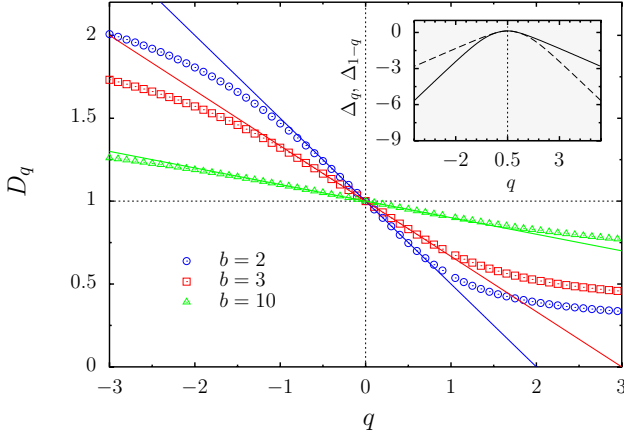


FIG. 2: (Color online) Fractal dimension D_q computed with the canonical method for $\gamma = 1/b$ with $b = 2$ (blue circles), $b = 3$ (red squares), $b = 10$ (green triangles). Solid lines show the linear approximation $D_q = 1 - q/b$. Inset: anomalous exponent Δ_q as a function of q (solid line), together with its symmetry with respect to $q = 1/2$ (dashed line) for $b = 2$.

is increased, Eq. (5) is verified with higher and higher accuracy. Of course Eq. (5) breaks down for large $|q|$ since D_q is bounded.

To get an understanding of why formula (5) holds, we note that general arguments for critical systems predict that the multifractal properties of the eigenstates for $q = 2$ are linked to the spectral statistics through a relation between the correlation dimension D_2 and the level compressibility χ [14],

$$\chi = \frac{1}{2} \left(1 - \frac{D_2}{D_0} \right). \quad (6)$$

Numerical results for the power-law random banded matrix ensemble [5] have revealed that this relation is extremely well verified in the regime of weak multifractality (large bands): in this model, the fractal dimension evolves linearly with respect to q as $D_q = 1 - \kappa q$, where κ is inversely proportional to the width of the central band (and in this particular case can be also related to the level compressibility). However, for smaller bands Eq. (6) was clearly violated. Suppose Eq. (6) holds in our case. For ISRM (Eq. (1)), the level compressibility can be estimated analytically. It is given by the value of the two-point correlation form factor $K_2(\tau) = |\text{Tr } U^n|^2/N$, with $\tau = n/N$, for $n/N \rightarrow 0$. Following [8], we note that in the semiclassical limit $N \rightarrow \infty$ and fixed n , the trace $\text{Tr } U^n$ is asymptotically equal to $\text{Tr } V_n$, where V_n is the quantization of the n th iterate of the classical map, and

$$\text{Tr } V_n = \frac{1}{N} \sum_{p=0}^{N-1} \exp(in\phi_p) \sum_{k=0}^{N-1} \exp(2i\pi n\gamma k). \quad (7)$$

The modulus squared of the first sum yields $\approx N$ when all ϕ_p are random. The second sum is a geometric sum:

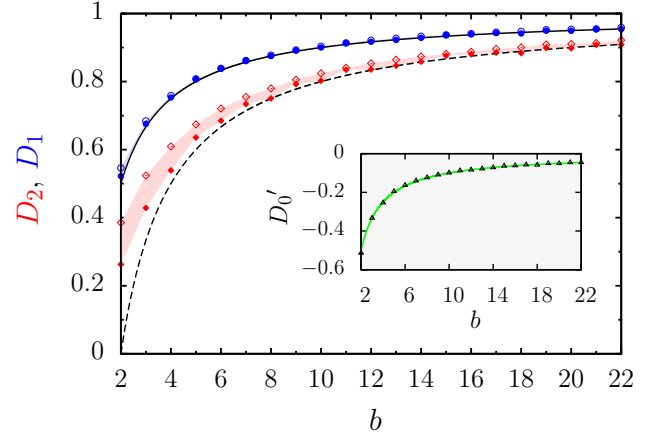


FIG. 3: (Color online) Information dimension D_1 (blue circles) and correlation dimension D_2 (red diamonds) as a function of the denominator of $\gamma = 1/b$. Full (empty) symbols are numerical values obtained by the method of moments (the canonical method). Solid and dashed lines are the theoretical curves $1 - 1/b$ and $1 - 2/b$ for D_1 and D_2 respectively. The values obtained by e.g. the box counting method lie in the shaded domain in between. Inset: slope of D_q at the origin $q = 0$ (triangles) and curve $-1/b$ (solid line).

for $\gamma = a/b$, it is equal to N if n is divisible by b and to $O(1)$ otherwise. Thus, $K_2(n/N) \sim 1$ provided n is divisible by b , $K_2(n/N) \sim 0$ in all other cases. The level compressibility is then given by the time averaged form factor

$$\chi = \overline{K_2(0)} \equiv \lim_{n \rightarrow \infty} \lim_{N \rightarrow \infty} \frac{1}{n} \sum_{n'=1}^n K_2(n'/N) \approx \frac{1}{b}. \quad (8)$$

Inserting this value of χ into Eq. (6) we get $D_2 \approx 1 - 2/b$, which corresponds to Eq. (5) for $q = 2$. A simple linear interpolation between this value for D_2 and $D_0 = 1$ yields Eq. (5). We note that for small b (strong multifractality) Eq. (6) breaks down but Eq. (5) is still valid for smaller q values.

Before moving to the study of the singularity spectrum, we briefly discuss symmetry properties of D_q . It was suggested in [6] that the anomalous exponents Δ_q , defined by $\Delta_q \equiv (D_q - 1)(q - 1)$, approximately follow the symmetry relation $\Delta_q = \Delta_{1-q}$. This was shown to hold for the Anderson model with good accuracy over a large interval of q values. It is not the case in our system. As an example, the inset in Fig. 2 gives Δ_q and Δ_{1-q} for $\gamma = 1/2$. For values of q where the exponents D_q have a linear behavior the symmetry relation holds, as it should since any linear D_q necessarily fulfills it. Outside the linear regime, the relation is not verified anymore.

We now turn to the singularity spectrum $f(\alpha)$. For $\gamma = a/b$, the expression obtained using Eq. (5) is

$$f(\alpha) \approx 1 - \frac{b}{4} \left(\alpha - 1 - \frac{1}{b} \right)^2. \quad (9)$$

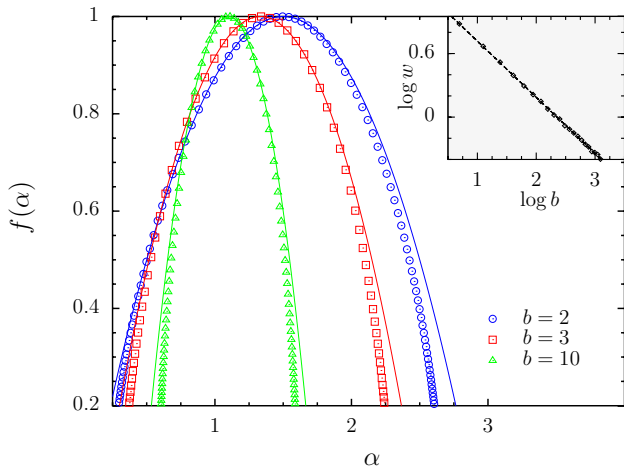


FIG. 4: (Color online) Singularity spectrum $f(\alpha)$ for $\gamma = 1/b$ with $b = 2$ (blue circles), $b = 3$ (red squares), $b = 10$ (green triangles). Solid lines show the parabola (9). Inset: singularity spectrum width $w = \alpha_{\max} - \alpha_{\min}$ as a function of b . The dashed line shows the best linear fit $\log w = -0.530 \log b + 1.247$. Logarithm is natural.

It reaches its maximum at $\alpha(q = 0) = 1 + 1/b$. Since Eq. (5) is valid around $q = 0$, we expect Eq. (9) to be accurate around $\alpha(0)$. Figure 4 shows the singularity spectrum, numerically computed using Eq. (4), together with the theoretical estimate Eq. (9). The data displayed show that (9) approximates the singularity spectrum with good accuracy over a large interval of values of α around $\alpha(0)$. As $b \rightarrow \infty$, the curve for $f(\alpha)$ gets closer and closer to a single point at $\alpha = 1$, once again corresponding to the non-fractal case of RMT.

We previously showed that the theory (5) accurately describes the behavior of the moments in Eq. (2) for small q . For large values of q , this is bound to break down since D_q converges to a finite asymptotic value for $q \rightarrow \pm\infty$. Similarly $f(\alpha)$ should have vertical asymptotes at some limiting values α_{\max} and α_{\min} , while (9) is the equation of a parabola. However numerical data are not far from the theory (9), and some of the features of $f(\alpha)$ are well captured by this estimate. For example, the inset of Fig. 4 shows that the width $w = \alpha_{\max} - \alpha_{\min}$ of the singularity spectrum scales as $\sim 1/b^{0.53}$ (best fit). This is close to the scaling $1/\sqrt{b}$ of the difference between the two intersections of the parabola (9) with a straight line.

We finish by noting that in the symmetric case ($\phi_{N-p} = \phi_p$ in Eq. (1)) we have performed similar computations, getting very similar data. In particular, Eqs. (5) and (9) are valid in this case as well.

In conclusion, we have studied multifractal properties of eigenfunctions for intermediate quantum maps. Although data corresponding to system sizes N with different values of $aN \bmod b$ should be treated separately,

they give the same value for D_q and $f(\alpha)$. Our results show that for an interval of q values whose size increases with b , the fractal exponents can be related explicitly to the parameter $\gamma = a/b$ of the map through Eq. (5), and thus to spectral statistics. A similar result holds for the singularity spectrum through Eq. (9). Thus in such a system, fractal exponents and singularity spectrum are related to the spectral properties over a wide range of fractal dimensions. Interestingly enough, our relation is still valid for small q even when Eq. (6) for $q = 2$ does not hold. As our system corresponds to a Random Matrix model covering the whole range of semi-Poisson statistics, both at short-range and long-range, we can expect our results to display some generality. It will be interesting to study if similar results apply to other intermediate systems, and other physical systems where wave functions are multifractal, such as condensed-matter systems at the Anderson or quantum Hall transitions.

We thank E. B. Bogomolny and K. Frahm for helpful discussions, CalMiP and IDRIS for access to their supercomputers, and the French ANR (project INFOSYSQQ) and the IST-FET program of the EC (project EUROSQIP) for funding.

-
- [1] F. Haake, *Quantum Signatures of Chaos* (Springer, Berlin, 1991).
 - [2] B. I. Shklovskii, B. Shapiro, B. R. Sears, P. Lambrianides, and H. B. Shore, Phys. Rev. B **47**, 11487 (1993); D. Braun, G. Montambaux, and M. Pascaud, Phys. Rev. Lett. **81**, 1062 (1998).
 - [3] E. B. Bogomolny, U. Gerland, and C. Schmit, Phys. Rev. E **59**, R1315 (1999); E. Bogomolny, O. Giraud and C. Schmit, Phys. Rev. E **65**, 056214 (2002).
 - [4] F. Evers and A. D. Mirlin, Phys. Rev. Lett. **84**, 3690 (2000); A. D. Mirlin, Phys. Rep. **326**, 259 (2000).
 - [5] E. Cuevas, M. Ortuno, V. Gasparian and A. Perez-Garrido, Phys. Rev. Lett. **88**, 016401 (2001); A. M. Garcia-Garcia and J. Wang, Phys. Rev. Lett. **94**, 244102 (2005).
 - [6] A. D. Mirlin, Y. V. Fyodorov, A. Mildenberger, and F. Evers, Phys. Rev. Lett. **97**, 046803 (2006).
 - [7] B. Huckestein, Rev. Mod. Phys. **67**, 357 (1995).
 - [8] O. Giraud, J. Marklof and S. O'Keefe, J. Phys. A **37**, L303 (2004).
 - [9] E. Bogomolny and C. Schmit, Phys. Rev. Lett. **93**, 254102 (2004).
 - [10] E. Bogomolny, private communication.
 - [11] A. Chhabra and R. V. Jensen, Phys. Rev. Lett. **62**, 1327 (1989).
 - [12] O. Giraud and B. Georgeot, Phys. Rev. A **72**, 042312 (2005).
 - [13] As U is not defined for $aN = 0 \bmod b$, dimensions N are not necessarily the same for all b .
 - [14] J. T. Chalker, V. E. Kravtsov and I. V. Lerner, JETP Letters **64**, 386 (1996).